OPEN

npg

Long-term cultured mesenchymal stem cells frequently develop genomic mutations but do not undergo malignant transformation

Y Wang[1,5], Z Zhang[2,5], Y Chi[1], Q Zhang[2], F Xu[1], Z Yang[1], L Meng[1,3], S Yang[1], S Yan[4], A Mao[4], J Zhang[4], Y Yang[2], S Wang[2], J Cui[1], L Liang[4], Y Ji[1], Z-B Han*[1,3,4], X Fang*[2] and ZC Han*[1,3,4]

Cultured human umbilical cord mesenchymal stem cells (hUC-MSCs) are being tested in several clinical trials and encouraging outcomes have been observed. To determine whether *in vitro* expansion influences the genomic stability of hUC-MSCs, we maintained nine hUC-MSC clones in long-term culture and comparatively analyzed them at early and late passages. All of the clones senesced in culture, exhibiting decreased telomerase activity and shortened telomeres. Two clones showed no DNA copy number variations (CNVs) at passage 30 (P30). Seven clones had ≥ 1 CNVs at P30 compared with P3, and one of these clones appeared trisomic chromosome 10 at the late passage. No tumor developed in immunodeficient mice injected with hUC-MSCs, regardless of whether the cells had CNVs at the late passage. mRNA-Seq analysis indicated that pathways of cell cycle control and DNA damage response were downregulated during *in vitro* culture in hUC-MSC clones that showed genomic instability, but the same pathways were upregulated in the clones with good genomic stability. These results demonstrated that hUC-MSCs can be cultured for many passages and attain a large number of cells, but most of the cultured hUC-MSCs develop genomic alterations. Although hUC-MSCs with genomic alterations do not undergo malignant transformation, periodic genomic monitoring and donor management focusing on genomic stability are recommended before these cells are used for clinical applications.

Genomic stability has a crucial role in stem cell-based therapies and has attracted much attention. Previous studies reported that embryonic stem cells (ESCs) commonly develop chromosomal abnormalities or DNA copy number variations (CNVs) during cultivation.[1,2] It is also difficult for induced pluripotent stem cells (iPSCs) to maintain genomic stability during reprogramming that is associated with the deletion of tumor suppressor genes.[3] Human umbilical cord mesenchymal stem cells (hUC-MSCs) are stem cells in an intermediate state of differentiation between ESCs and adult stem cells. The differentiation and immunoregulatory capabilities of hUC-MSCs make them candidates for treating several refractory diseases.[4,5] Cultured hUC-MSCs are being tested in several clinical trials (www.clinicaltrials.gov), and encouraging outcomes have been observed.[6–8] Because of the high frequency of

genomic mutations during long-term passaging of ESCs and iPSCs, it is necessary to determine whether hUC-MSCs, such as ESCs and iPSCs, can be grown indefinitely in culture and undergo adaptive genetic changes during the long-term expansion.

Aneuploidy was observed in *in vitro*-cultured bone marrow MSCs (BMMSCs) and adipose tissue-derived MSCs (ADMSCs). Aneuploidy could be found not only at the late passage but also at early passages of *in vitro* culture.[9–11] Limited by the resolution of traditional karyotyping, it is not the most effective method for evaluation of genomic stability of MSCs for clinical applications. Some studies analyzed CNVs of *in vitro*-cultured BMMSCs and ADMSCs. Nonetheless, for the relatively shorter *in vitro* life span of BMMSCs and ADMSCs, few *in vitro* culture-related CNVs were found in

[1]State Key Laboratory of Experimental Hematology, National Engineering Research Center of Stem Cells, Institute of Hematology and Hospital of Blood Diseases, Chinese Academy of Medical Science and Peking Union Medical College, Tianjin, China; [2]Laboratory of Disease Genomics and Individualized Medicine, Beijing Institute of Genomics, Chinese Academy of Sciences, Beijing, China; [3]TEDA Life Science and Technology Research Center, Institute of Hematology, Chinese Academy of Medical Science, Tianjin, China and [4]National Engineering Research Center of Cell Products/AmCellGene Co. Ltd, Tianjin, China
*Corresponding authors: ZC Han or Z-B Han, State Key Laboratory of Experimental Hematology, National Engineering Research Center of Stem Cells, Institute of Hematology and Hospital of Blood Diseases, Chinese Academy of Medical Science and Peking Union Medical College, 288 Nanjing Road, Tianjin 300020, China. Tel: +86 022 6621 1206; Fax: +86 022 6621 1430; E-mail: hanzhongchao@hotmail.com (ZCH) or zhibohan@163.com (Z-BH)
or X Fang, Laboratory of Disease Genomics and Individualized Medicine, Beijing Institute of Genomics, Chinese Academy of Sciences, No.1-7 Beichen West Road, Chaoyang, Beijing 100101, China. Tel: +86 10 8409 7495; Fax: +86 10 8409 7720; E-mail: fangxd@big.ac.cn
[5]These two authors contributed equally to this work.

these studies.[12–14] Whether MSCs with genomic instability undergo malignant transformation in culture or could form a tumor in an animal model was not clear.

In the present study, we maintained hUC-MSCs in vitro until the senescent stage and performed high-resolution array-based comparative genomic hybridization (aCGH) using nine pairs of hUC-MSC clones (late passages versus early passage). Multipotency, cell surface markers, telomere length, telomerase activity and in vivo tumorigenesis were also analyzed. Furthermore, we used mRNA-Seq analysis to identify the differences in gene expression profiles between genomically stable and unstable hUC-MSC clones, particularly during the transition from an early to a late passage.

Results

hUC-MSC preparation and long-term cultivation.
hUC-MSCs from nine hUCs obtained from healthy donors were isolated as described previously.[15] The hUC-MSCs were harvested using trypsin after reaching 90% confluence and subplated at a 1 : 3 ratio until reaching a senescence phase. After a period of proliferation, all nine clones entered a senescence phase and stopped growing. The cells were counted at passages 3 (P3) and 30 (P30). On average, the hUC-MSC population of the nine hUC-MSCs clones expanded by the factor of 4.65×10^{12} from P3 to P30 in this study. In fact, we originally maintained 24 hUC-MSC clones from different donors. All of them became senescent in culture, with different life spans in vitro (Supplementary Figure 1). The average life span of the 24 clones was 31.7 passages. No immortalization was observed in this study.

Demonstration of the absence of cross-contamination during hUC-MSC cultivation.
Recent research on genomic stability and spontaneous malignant transformation of MSCs during long-term cultivation gave rise to conflicting findings. Genomic changes and malignant transformation observed during the cultivation of BMMSCs in vitro was suspected to be a cross-contamination artifact.[16–19] The short tandem repeat (STR) profile of transformed MSCs was not compatible with that of the original MSCs but was quite similar to that of some tumor cell lines that were available in the laboratory.[17] To minimize the probability of cross-contamination, all cell culture procedures of this study were in compliance with the guidelines of current good manufacturing practices. There were no exogenous tumor cells in the clean room where the long-term hUC-MSC culture was maintained. Furthermore, the STR analysis was used to confirm that the paired early- and late-passage hUC-MSCs were derived from the same individual. The loci in our STR analysis contained 15 CODIS (Combined DNA Index System) STR loci, which have been successfully used for individual identification in forensic sciences.[20] If any early- and late-passage samples have matching genotypes at all CODIS loci, it is a virtual certainty that the two DNA samples came from the same individual, and thus we could conclude that there was no cross-contamination in the cell culture. In the current study, each hUC-MSC clone had a unique and unchanged STR profile at P3 and P30, indicating the absence of cross-contamination (Supplementary Table 1).

Multipotency of hUC-MSCs after long-term culture.
hUC-MSCs at P30 were negative for CD11b, CD19, CD34, CD45, and HLA-DR, and were positive for CD29, CD44, CD73, CD90, CD105, and HLA-ABC (Supplementary Figure 2). The hUC-MSCs expressed multipotent stem cell markers Nestin and Sox2 at both early and late passages, and could be induced to undergo adipogenesis and osteogenesis under lineage-specific culture conditions (Figures 1a, b, and c). Previous studies have shown that Nestin (+) MSCs constituted an essential HSC niche component and can be propagated as nonadherent 'mesenspheres' that can self-renew and expand in serial transplants,[21] whereas Sox2(+) stem cells are crucial for normal tissue regeneration and survival.[22] These results showed that hUC-MSCs maintained their multipotency after the long-term culture in vitro.

Senescence, telomerase, and telomere length of hUC-MSCs during cultivation.
In in vitro culture, particularly at the late passages before senescence, the cell size increased, whereas the growth rate decreased and ultimately reached zero. Senescence of hUC-MSCs at late passages can be determined by the appearance of senescence-associated β-galactosidase activity (Figure 1d). Abnormal morphology and smaller cell size (Figure 1e) appeared sometimes in the culture of late passages. Despite the increased proliferation rate, the smaller cells could not escape senescence, which was similar to BMMSCs in Bernardo's study.[13] After a period of rapid proliferation, these smaller cells also became senescent.

All of the nine clone pairs analyzed in this study expressed the gene of human telomerase reverse transcriptase (hTERT), that is, the human telomerase catalytic subunit, at early passage. The hTERT expression level in hUC-MSCs was 1% lower than that in HeLa cells (Supplementary Table 2). hTERT expression in hUC-MSCs decreased during in vitro culture (Figure 2a) and became undetectable in many hUC-MSC clones at the late passage. Furthermore, a Southern blot-based assay revealed that telomere length in hUC-MSCs decreased from early to late passages (Figures 2b and c). These results indicated that the weak telomerase activity in hUC-MSCs could not maintain the telomere length in in vitro culture.

CNV and karyotype analysis during long-term cultivation.
Genomic stability of the nine clone pairs (the early (P3) and late (P30) passages) was assessed using aCGH and traditional karyotyping. Of the nine pairs, two showed no CNV at the late passage and the other seven had ≥ 1 detectable CNVs at the late passage compared with the corresponding early-passage clones (Figure 3a and Table 1). The distribution of CNVs among the hUC-MSC clones was unequal. Significant differences in genomic stability were observed among the clones (Figures 3b and c). Similarly, the distribution of CNVs among different chromosomes was also unequal (Figures 3d and e). A total of 285 CNV segments were observed among the seven hUC-MSC clones at the late passage. In total, 204 CNV segments were amplified, whereas the other 81 CNV segments were deleted. Thus, CNV amplification was more likely to occur than deletion during in vitro cultivation. However, there is a possibility that
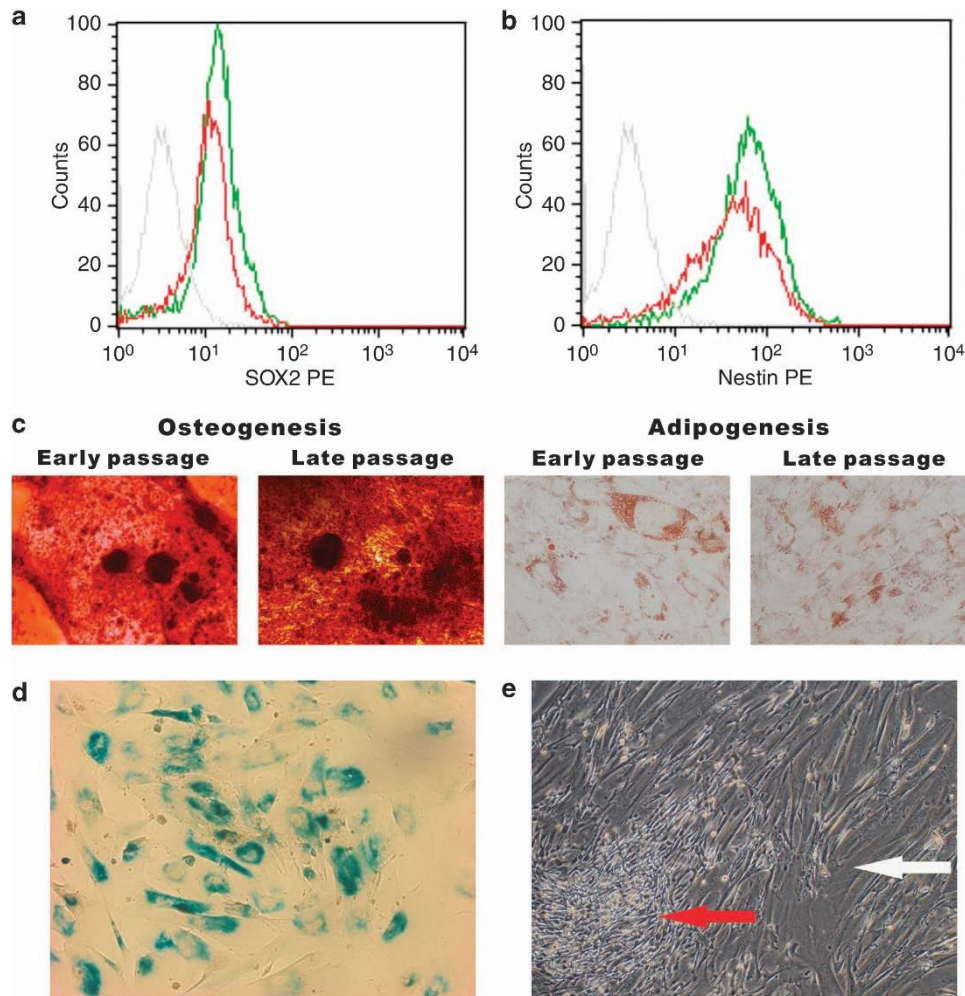
Figure 1 Characterization of hUC-MSCs. Nestin (**a**) and Sox2 (**b**) expression in hUC-MSCs at P3 (red) and P30 (green) was analyzed by flow cytometry. Osteogenic and adipogenic differentiation were visualized using Alizarin Red and Oil Red O staining at early and late passages (**c**) separately. Senescence-associated β-galactosidase activity was observed in hUC-MSCs at the late passage (**d**). hUC-MSCs with smaller size and rapid proliferation (**e**, red arrow) were distinct from the senescent cells with a flat morphology (**e**, white arrow)

hUC-MSCs with CNV amplification gained a growth advantage over hUC-MSCs with CNV deletions. CNVs observed in this study ranged from 12 kb to 1.3 Mb. The average and median size of CNVs were 67 and 27 kb, respectively. Unlike ESCs or iPSCs, in hUC-MSCs, CNVs observed were shorter than 10 Mb and might exist only in a subpopulation of the culture, indicating that gene expression-based methods are not suitable for the detection of small genomic aberrations of hUC-MSCs arising during cultivation.[3,23] Compared with traditional karyotype analysis and gene expression-based methods, aCGH provides enough resolution and might be the best method to evaluate genetic changes in hUC-MSCs from early to late passages. Karyotype analysis revealed that eight of the nine hUC-MSC clones retained normal karyotype during *in vitro* expansion. Trisomy for chromosome 10 was found in clone 6 at P30 (Figures 4a and b and Supplementary Figure 3), which was consistent with the results of aCGH. The rainbow plot (Figure 4c) showed that most of the segments on chromosome 10 of clone 6 at P30 were amplified compared with clone 6 at P3.

The clones with most CNV segments at P30 (i.e., clone 3) were further analyzed by aCGH at P10 and P20. Some CNVs detected at P30 could not be found at P10 or P20. Conversely, some CNVs detected at P10 or P20 could not be found at P30 (Supplementary Figure 4). A rational explanation for this phenomenon is that hUC-MSCs with detectable mutations usually acquire a growth advantage, so that CNVs at the late passage can be found using aCGH. On the other hand, if the growth advantage provided by CNVs was not so strong and persistent so as to help the cells to dominate the population, then the CNVs could appear and then disappear in the course of cultivation. Of note, the hUC-MSC clone without CNVs at P30 (clone 8) had 25 CNV segments when analyzed at P10 (Supplementary Figure 5), suggesting that genomic changes might be inevitable in the long-term hUC-MSC culture.

To determine whether some regions of the genome were prone to CNVs during *in vitro* cultivation, in Supplementary Table 3, we listed the segments that underwent CNVs in two or three hUC-MSC clones during the prolonged expansion. Twenty-five CNV segments were found in $\geqslant 2$ clones. Three segments
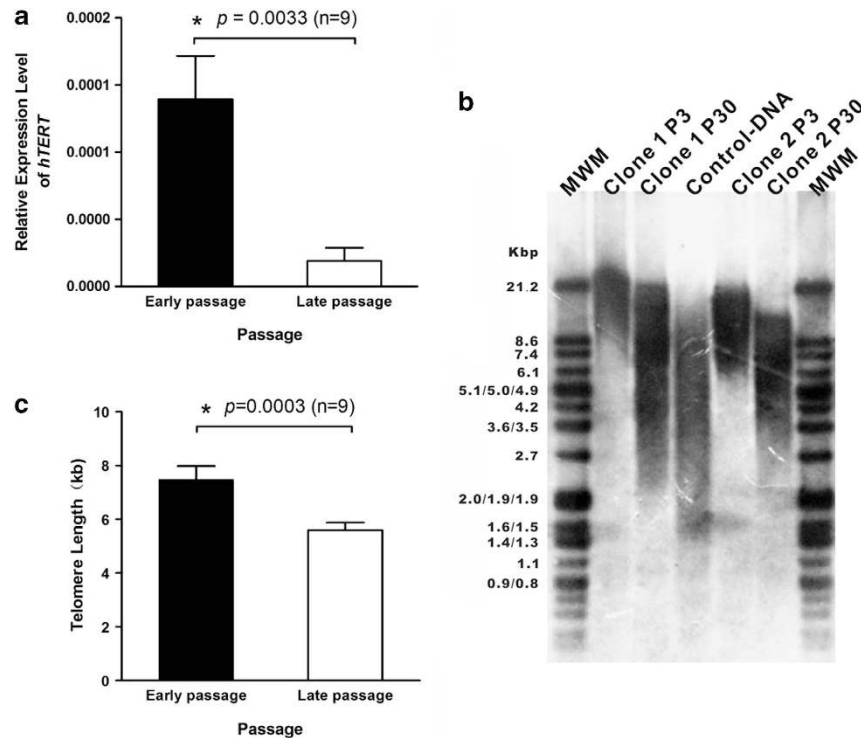
Figure 2 Telomerase and telomere analysis. (**a**) Analysis of *hTERT* expression in hUC-MSCs at early and late passages. Relative expression levels were calculated using the $-\Delta\Delta$Ct method in comparison with those of HeLa cells. (**b**) Telomere length analysis of two hUC-MSC clones at early and late passages using Southern blotting. A reduction in telomere length was observed in hUC-MSCs from early to late passages. The control DNA supplied with the *TeloTAGGG* Telomere Length Assay Kit was genomic DNA purified from immortalized cell lines. MWM, molecular weight marker. (**c**) Telomere length of nine pairs of hUC-MSC clones at early and late passages. A paired *t*-test was used in the analysis of telomere length and *hTERT* expression in hUC-MSCs at early and late passages. Statistical analysis revealed that the telomere length of hUC-MSCs at the late passage was significantly shorter than that at early passage

(chr11 : 64900602, 64945906; chr16 : 30107502, 30124017; and chr20 : 62041966, 62064408) were shared by three clones. These results indicated that there might be some chromosomal regions in which CNVs arose more frequently in the *in vitro* culture. Some genes (*CORO1A*, *BOLA2B*, *SLX1B*, and *SLX1A*) in these mutation-prone chromosomal regions are involved in cell proliferation or cell cycle regulation, DNA repair, or DNA recombination processes. No CNV segment was found in four or more hUC-MSC clones.

Tumorigenesis *in vivo*. Next, we wanted to test whether hUC-MSCs that acquired CNVs or aneuploidy during long-term culture underwent malignant transformation. Three hUC-MSC clones containing CNVs (including the clone containing trisomy for chromosome 10) at P30 and two clones without CNV at P30 were assessed in an immunocompromised mouse model of tumorigenesis in comparison with a human ESC line, H1. Female SCID mice were inoculated *s.c.* with 500 μl Matrigel containing 4×10^6 hUC-MSCs. Eight weeks after injection, no sign of tumor development was observed in the mice that received hUC-MSCs, regardless of the presence of CNVs or aneuploidy at the late passage (Figures 5a and c). In contrast, typical teratoma developed in the mice injected with ESCs (Figures 5b, d, e, and f) 2 weeks after inoculation. These results indicated that a tumor did not develop after a transplant of hUC-MSCs, even if those cells had obvious genetic alterations.

Assessment of transcript expression using mRNA-Seq and pathway analysis. To compare gene expression profiles of genomically stable hUC-MSCs and unstable hUC-MSCs, we performed mRNA-Seq for three pairs (early and late passages) of hUC-MSC clones: clone 8 (without CNV at the late passage), clone 2 (with slight CNVs at the late passage), and clone 6 (trisomic for chromosome 10 and with many CNVs at the late passage) using the Hi-seq 2000 Genome Analyzer platform (Illumina, San Diego, CA, USA). Fragments per kilobase of transcript per million mapped reads (FPKM) were used to estimate transcript abundance. To determine differentially expressed genes, the genes with statistically significant difference of FPKM values were selected following the criteria of fold change >2 and $P < 0.05$. The expression of most genes in mRNA-Seq analysis was consistent with that in real-time PCR (RT-PCR) analysis (Supplementary Figure 6), suggesting that we obtained an acceptable data set of transcripts expressed in the tested cells. Unsupervised hierarchical clustering of genome-wide expression profiles was performed to assess similarity of the transcriptome among these six clones (Figure 6). We observed that the clones could be subdivided into two distinct groups: cells with normal or slight CNVs (clone 2 P3, clone 8 P3, clone 8 P30, clone 2 P30, and clone 6 P3) and cells containing large-scale chromosomal changes (clone 6 P30). Clone 2 P3 and clone 8 P3 were highly correlated and different from clone 6 P3, although all of them were
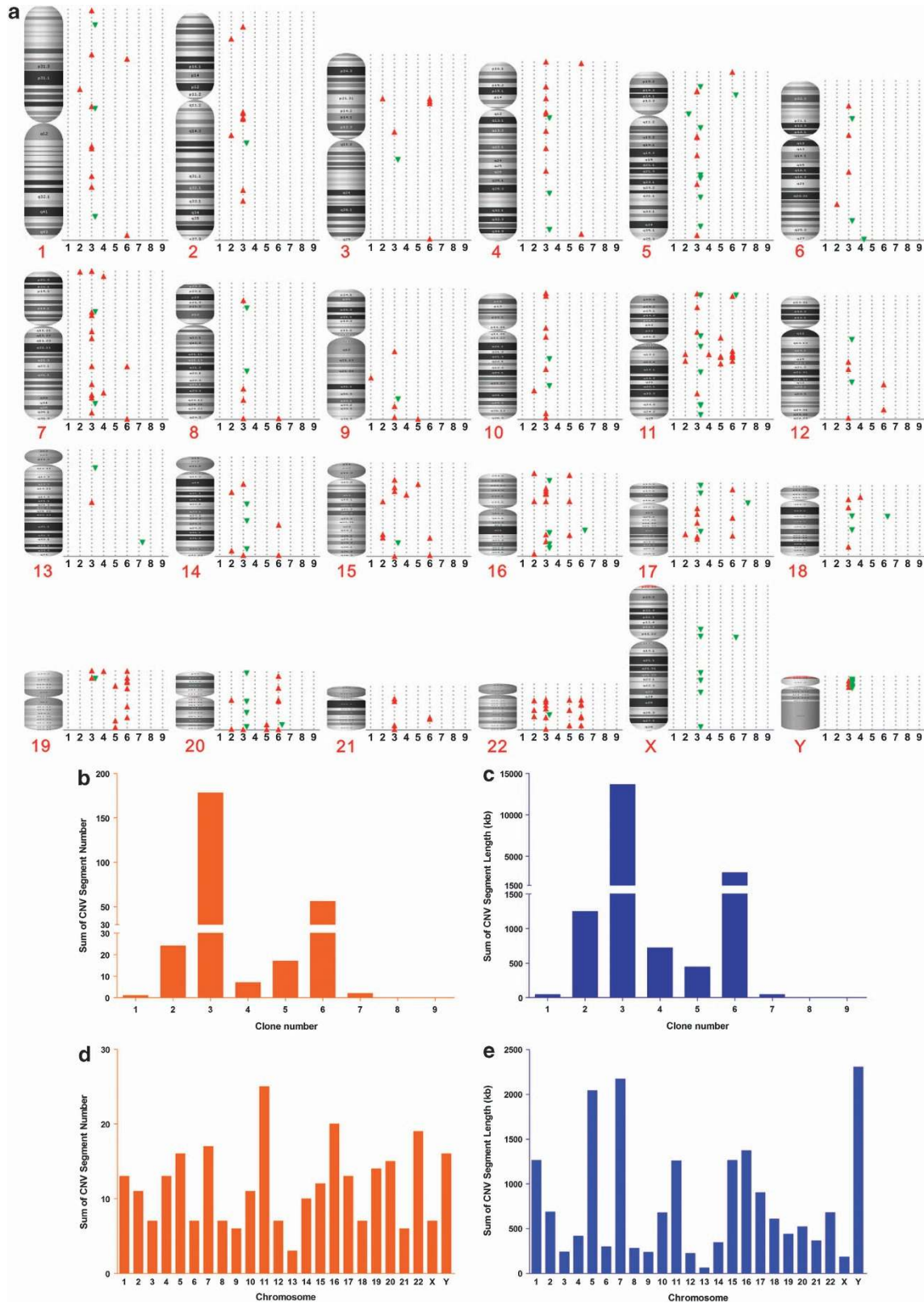
Figure 3 CNVs identified by aCGH in culture. (**a**) Amplifications and deletions were mapped onto the human genome for nine hUC-MSC clones at P30 *versus* P3. Trisomy for chromosome 10 in clone 6 was not considered CNV, and thus is not shown in this figure. Each individual CNV is marked with a symbol: ▲, amplification; ▼, deletion. CNV segment number and length for each hUC-MSC clone are presented in panels **b** and **c**, respectively. CNV segment number and length for each chromosome are shown in panels **d** and **e**, respectively

Table 1 Summary of CNV segments occurring during hUC-MSC cultivation

Clone ID	Number of CNV segments	Sum of length (kb)	Average length (kb)	Deletion			Amplification		
				Number	Sum of length (kb)	Average length (kb)	Number	Sum of length (kb)	Average length (kb)
1	1	42	42	0	0	0	1	42	42
2	24	1246	52	1	83	83	23	1163	51
3	177	13653	77	71	3010	42	106	10642	100
4	7	721	103	1	19	19	6	702	117
5	17	444	26	0	0	0	17	444	26
6	56	3030	54	6	212	35	50	2819	56
7	2	41	21	2	41	21	0	0	0
8	0	0	0	0	0	0	0	0	0
9	0	0	0	0	0	0	0	0	0

Abbreviations: aCGH, array-based comparative genomic hybridization; CNV, copy number variation; hUC-MSC, human umbilical cord mesenchymal stem cells
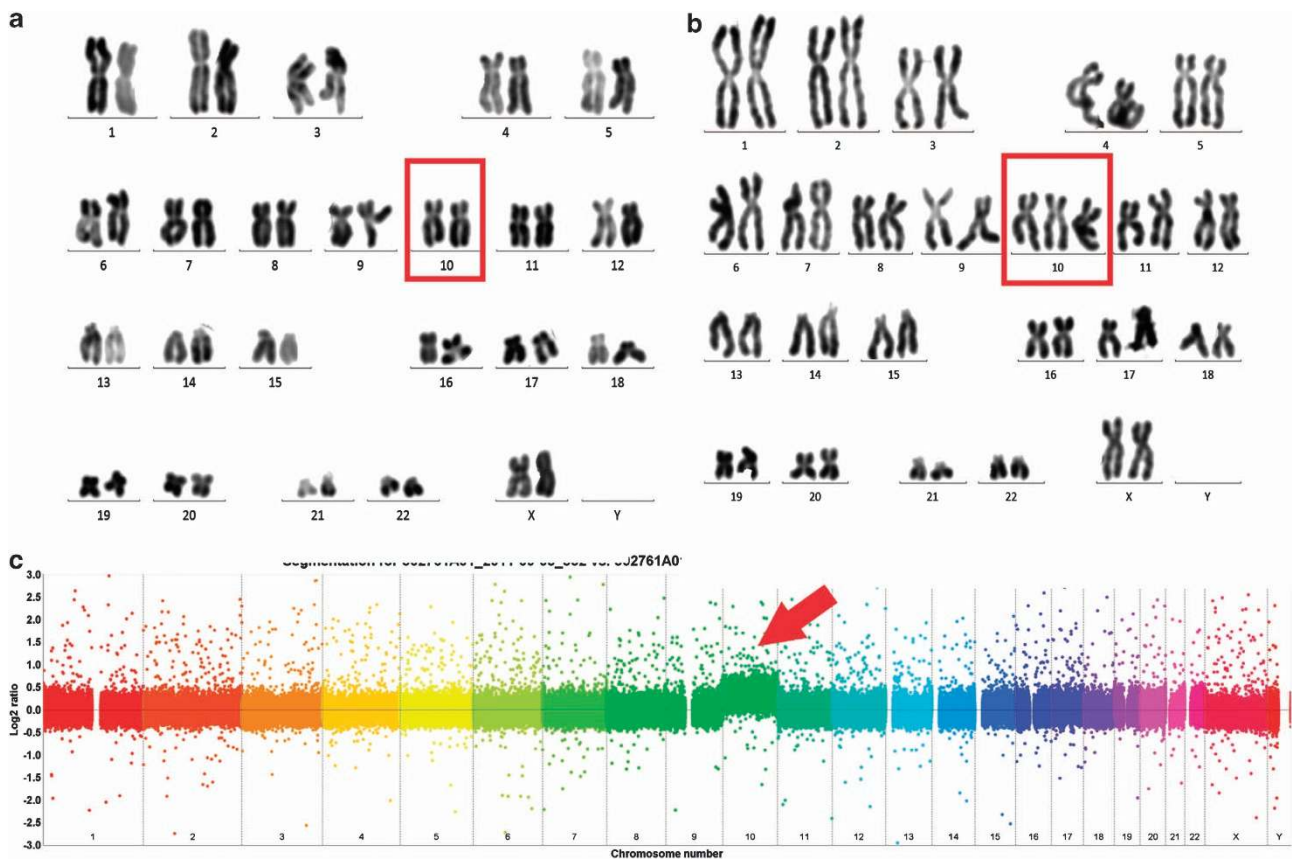The CNV data on nine paired clones (P30 *versus* P3) were derived from aCGH

Figure 4 Genetic changes observed in long-term cultured hUC-MSCs. (**a**) R-banded karyotype of clone 6 P3 with a normal chromosomal number. (**b**) R-banded karyotype of clone 6 P30 with trisomy for chromosome 10 (red box). (**c**) aCGH analysis of clone 6 P30 displayed as a single-panel rainbow plot with each chromosome differentiated by color. The red arrow shows the amplifications on chromosome 10

early-passage (P3) hUC-MSCs. On the other hand, clone 6 P3 showed a strong correlation with clone 2 P30, which was a late-passage hUC-MSC sample with slight CNVs. This observation indicates that clone 6 P3 may already carry some aberrations that make it different from the other early-passage hUC-MSCs (clone 2 P3 and clone 8 P3).

Next, we attempted to determine the change in the biological functions of the hUC-MSCs with genetic alterations using clone 6 P3, clone 2 P3, and clone 8 P3 ($P < 0.05$, fold change of >2). According to Gene Ontology annotations of genes that were expressed significantly higher in the genomic-unstable sample clone 6 P3 compared with clone 2 P3 and clone 8 P3, 14.7% genes enriched in Gene Ontology annotations were associated with cell cycle, 13.5% were associated with cancer and 10.9% were associated with cellular motility. These data were consistent with the pathway and network analyses using the same gene data sets (data not shown), indicating that clone 6 P3 was much more active
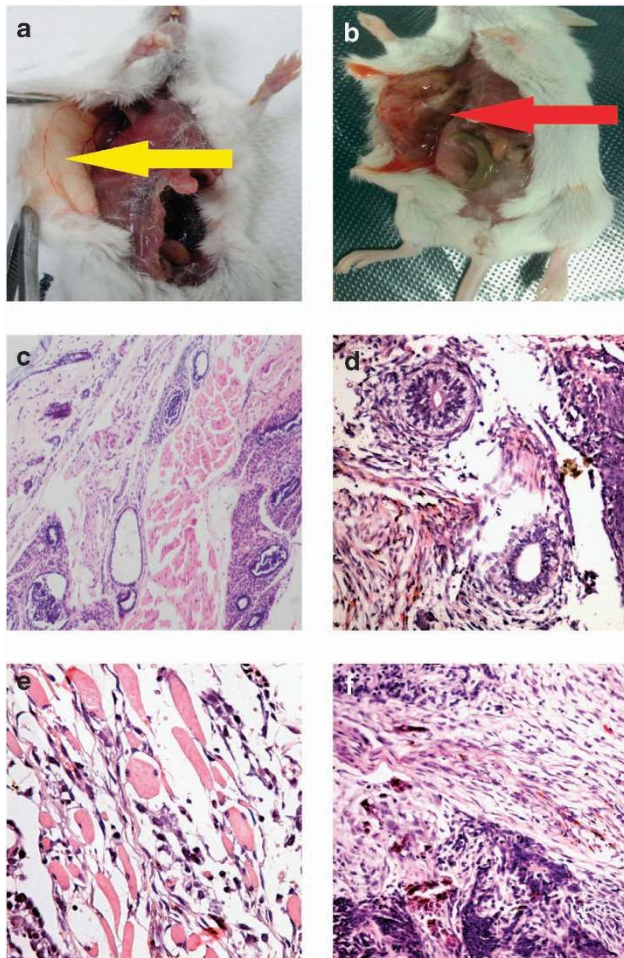
Figure 5 Long-term cultured hUC-MSCs did not generate malignant tumors in SCID mice. In the mice that received hUC-MSCs, no tumor was found in the subcutaneous tissues of the injection site (**a** and **c**). However, ESCs gave rise to a teratoma (**b**). Hematoxylin and eosin staining of the teratoma was performed. (**d**) Intestinal crypts (endoderm); (**e**) muscles (mesoderm); and (**f**) nerve fibers (ectoderm)

Figure 6 Unsupervised clustering of genome-wide gene expression (adjusted FPKM of >1) for six samples (clone 2 P3, clone 2 P30, clone 6 P3, clone 6 P30, clone 8 P3, and clone 8 P30). Clustering on the horizontal axis demonstrates two clusters: normal cells and cells with slight CNVs (clone 2 P3, clone 2 P30, clone 6 P3, clone 8 P3, and clone 8 P30) and cells containing substantial chromosomal changes (clone 6 P30)

than clone 2 P3 and clone 8 P3 in driving proliferation, cellular movement, as well as tumorigenesis. The core molecules of the networks (Supplementary Figure 7), including *CCND1*, *NFκB2*, *IL1B*, *IL6*, *CDK1*, and *PTGS2*, are mainly linked to the biological functions of cell cycle and immune response,[24–28] and may serve as biomarkers for the identification of hUC-MSCs with the genomic instability potential at early passages. These molecules may also be interesting because of possible clinical applications.

The Ingenuity Pathway analysis (IPA, http://www.ingenuity.com/) was performed to identify the biological functions of differentially expressed genes during cell passaging. We did not find any changed pathway shared by genetically normal (clone 8 without CNV) and abnormal clones (clone 2 and 6, both with CNV). Nonetheless, there were some overlaps in upregulated pathways between the clones with large chromosomal changes and those with slight CNVs (Table 2). Cell division tended to cause DNA mutations, particularly in *in vitro* cell culture. Some hUC-MSC clones
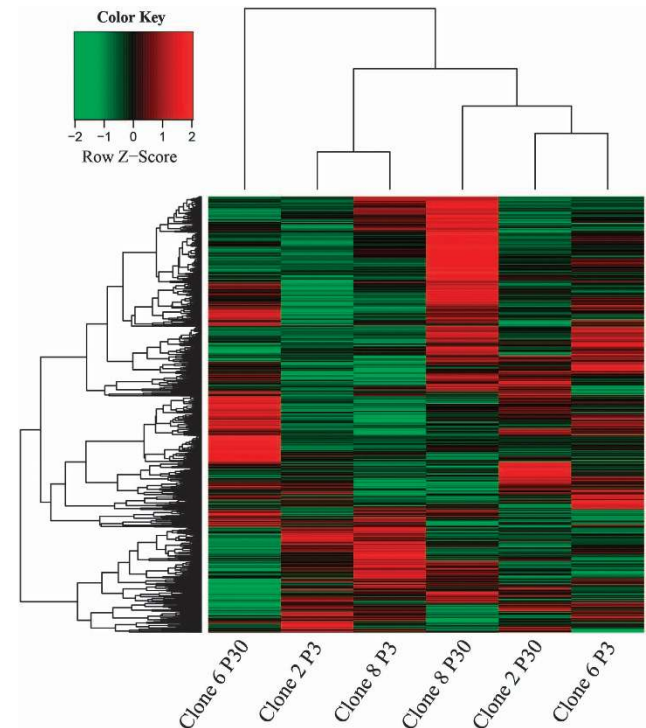
resisted the tendency of genomic instability during *in vitro* cultivation. In these clones, the pathways of cell cycle control and DNA damage response were upregulated during the prolonged expansion. Conversely, in the clones with substantial chromosomal changes, pathways of cell cycle control and DNA damage response were downregulated from early to late passages (Table 2).

Discussion

As a population of stem cells possessing great proliferation potential, hUC-MSCs are suitable for large-scale manufacture for clinical applications. Deposition of qualified hUC-MSCs into cell banks therefore offers unique opportunities to speed up clinical translation of stem cells to 'cell medicine' for both autologous and allogeneic therapies.[7,15] Because of the low frequency of MSCs in human tissues, the primary MSCs must be expanded extensively *in vitro* to achieve the quantity necessary for therapeutic purposes.[29–31] Before our study, many authors have reported contradicting results concerning the ability of MSCs to undergo spontaneous malignant transformation, with some investigators demonstrating that MSCs become tumor cells spontaneously during *in vitro* cultivation,[18,19,32] and others reporting that MSCs do not develop any genetic mutations nor do they undergo transformation after long-term culture.[13] Soon afterwards, the transformed MSCs were confirmed to be the result of

Table 2 Pathways of differentially expressed genes form early (P3) to late (P30) passages

Enriched genes	Pathways category	Clone 6	Clone 2	Clone 8
Upregulated	Atherosclerosis signaling	√		
Upregulated	Hepatic fibrosis/hepatic stellate cell activation	√		
Upregulated	HMGB1 signaling	√		
Upregulated	LXR/RXR activation	√		
Upregulated	TREM1 signaling;	√		
Upregulated	Role of macrophages, fibroblasts, and endothelial cells in rheumatoid arthritis	√	√	
Upregulated	Role of IL-17F in allergic inflammatory airway diseases		√	
Upregulated	Role of IL-17A in arthritis		√	
Upregulated	IL-17A signaling in fibroblasts		√	
Upregulated	Role of IL-17A in psoriasis		√	
Upregulated	Role of osteoblasts, osteoclasts, and chondrocytes in rheumatoid arthritis		√	
Upregulated	Coagulation system		√	
Upregulated	Differential regulation of cytokine production in macrophages and T-helper cells by IL-17A and IL-17F		√	
Upregulated	IL-17A signaling in airway cells		√	
Upregulated	**Cell cycle control of chromosomal replication**			√
Upregulated	**Role of BRCA1 in DNA damage response**			√
Upregulated	**Mitotic roles of polo-like kinase**			√
Upregulated	Hereditary breast cancer signaling			√
Upregulated	**Role of CHK proteins in cell cycle checkpoint control**			√
Upregulated	**ATM signaling**			√
Upregulated	Cyclins and cell cycle regulation			√
Upregulated	DNA double-strand break repair by homologous recombination			√
Upregulated	Cell cycle: G1/S checkpoint regulation			√
Upregulated	**Mismatch repair in eukaryotes**			√
Upregulated	Cell cycle: G2/M DNA damage checkpoint regulation			√
Downregulated	**Cell cycle control of chromosomal replication**	√		
Downregulated	**Mitotic roles of polo-like kinase**	√		
Downregulated	**Role of BRCA1 in DNA damage response**	√		
Downregulated	**Role of CHK proteins in cell cycle checkpoint control**	√		
Downregulated	**Mismatch repair in eukaryotes**	√		
Downregulated	**ATM signaling**	√		

Abbreviations: IL, interleukin; hUC-MSC, human umbilical cord mesenchymal stem cell
The text in bold in the table represents pathways that were upregulated in hUC-MSC clones with good genomic stability and downregulated in hUC-MSC clones with poor genomic stability during of *in vitro* culture

cross-contamination with tumor cell lines.[33–35] Acknowledging the error, we followed stringent working procedures and verified that the cells in our studies were not contaminated during the long-term *in vitro* culture. In this study, all of the hUC-MSC clones underwent a decrease in telomerase activity and shortening of telomere length and senesced in culture ultimately. No immortalization or malignant transformation was observed in the present study, which was consistent with the result observed in the study of BMMSCs.[13,36]

Previous researches paid much attention on the genomic stability of cultured MSCs. Based on traditional karyotype analysis, some studies found that abnormal karyotype appeared in the culture of ADMSCs and BMMSCs.[10,11,37] However, whether MSCs with genomic anomalies gained the ability of forming tumor *in vivo* was unclear, even though chromosomal aberrations were found in cultured ADMSCs and BMMSCs. High-throughput methods were also used to investigate the genomic mutation of cultured ADMSCs and BMMSCs,[12,14] whereas, these studies failed to find significant genomic changes and stated that MSCs expanded *in vitro* confirmed an overall stability of genomic profile. This might be because of the shorter *in vitro* life span of ADMSCs and BMMSCs, and thus the effect of prolonged culture on the genomic stability of MSCs could not be revealed sufficiently. The passage analyzed in our study was much later compared with the studies on BMMSCs or ADMSCs and also much later

than the passages that were used in clinical applications. Thus, the risks of cultured MSCs could be fully assessed in the present work. We found that hUC-MSCs frequently, and probably inevitably, underwent CNVs during *in vitro* culture. Furthermore, we analyzed the tumorigenesis of hUC-MSCs at late passage *in vivo*. According to our data, hUC-MSCs with genetic alterations, whether CNVs, or chromosomal number change, could not form a tumor in immunodeficient mice.

For lacking of obvious CNVs in previous high-throughput analysis, there is almost no knowledge about the difference between genomically stable and unstable MSC clones.[12–14] By analyzing the amount of CNV segments at the P30, different genomic instability was observed among hUC-MSCs derived from different donors in our study. To analyze the relationship between the transcriptome and genomic instability during prolonged culture of hUC-MSCs derived from different donors, we studied the genome-wide changes in gene expression, molecular networks, and signaling pathways for three pairs of hUC-MSC clones (at early and late passages) using the high-throughput sequencing technology. We found that genomically unstable hUC-MSCs showed abnormal expression profiles at early passage (P3). A set of genes, including *CCND1*, *NFκB2*, *IL1B*, *IL6*, *CDK1*, and *PTGS2*, that highly expressed in genomically unstable hUC-MSCs were identified at early passage. Detection of these genes might help to assess the potential risks of genomic

instability of hUC-MSCs at early passages. We also found that the pathways related to cell cycle control and DNA damage response showed specific changes during the long-term hUC-MSC culture. These pathways were definitely downregulated during the culture of hUC-MSCs with genomic instability; however, the same pathways were upregulated in normal clones with genomic stability. These observations suggest that perturbations of the above pathways could lead to the genomic instability of hUC-MSCs during long-term culture. Thus, the regulation of these pathways and the key genes in these pathways are factors critical for maintaining the genomic stability of hUC-MSCs during long-term culture. The state of these pathways or gene expression in hUC-MSCs may correlate with the cell culture state and genomic instability of hUC-MSCs, which resulted from chromosomal anomalies or changed epigenetic characteristics. Therefore, investigation of the pathways related to cell cycle control and DNA damage response will help to understand the process of hUC-MSC passaging and the molecular mechanisms underlying genomic stability.

Because CNVs or chromosomal number change has been found in a wide variety of human neoplastic tumors,[38–41] the potential tumorigenicity of MSCs with chromosomal abnormalities or CNV mutations cannot be completely ruled out. As the occurrence of genetic alterations during *in vitro* cultivation was relatively high and pathway related, the development of optimized culture methods will also be needed to stabilize the genome of stem cells during long-term cultivation. In addition, a combination of methods including long-term cultivation, aCGH, and pathway analysis should be used to analyze the genomic stability of hUC-MSCs. hUC-MSCs with few CNVs and with upregulation of DNA damage response may be safer and more suitable for the development of new medical treatments.

Materials and Methods

Preparation, long-term cultivation, and analysis of biological characteristics of hUC-MSCs. hUC-MSCs from nine hUC samples were isolated as described previously.[4,8] The cells were cultured in a monolayer at 37 °C and 5% CO_2 in DMEM/F12 (Gibco, Grand Island, NY, USA) with 10% fetal calf serum (ExCell Bio, Shanghai, China), harvested using trypsin (Gibco) after reaching 90% confluence, and subplated at a 1:3 ratio until reaching a senescence phase. The cell number was counted using Casy-TTC (Roche, Reutlingen, Germany). T75 cell culture flasks were used for *in vitro* culture. The population expansion was calculated as follows: (cell number in one flask at P30 × 3^(30−3))/cell number in one flask at P3. '30 − 3' means from P3 to P30. StemPro adipogenesis and osteogenesis differentiation kits (Gibco) were used to evaluate the differentiation potential of hUC-MSCs at early (P3) and late (P30) passages. Cell surface markers and Nestin and Sox2 expression were quantified using Calibur (BD Biosciences, Franklin Lakes, NJ, USA). Senescent cells were detected using a cellular senescence assay kit (Millipore, Billerica, MA, USA), according to the manufacturer's protocol. In the assay, senescence-associated β-galactosidase catalyzes the hydrolysis of X-gal, which results in the accumulation of a distinctive blue color in senescent cells.

STR analysis. We used a commercial STR kit, Goldeneye (Peoplespot Inc., Beijing, China)[42] to analyze the STR profiles of hUC-MSC clones at early and late passages and the absence of cross-contamination during long-term *in vitro* culture. The STR kit contained 15 STR loci (*vWA, D21S11, D18S51, PentaE, D5S818, D13S317, D7S820, D16S539, FGA, D3S1358, TH01, D8S1179, TPOX, CSF1PO,* and *PentaD*) and the sex marker *amelogenin*. Fluorescence labeling and repeat sequence for each STR locus are listed in Supplementary Table 4. Following the protocol, a PCR mixture containing 7 μl ddH$_2$O, 10 μl 2.5 × PCR buffer, 5 μl primer mixture, 0.5 μl Taq, and 2.5 μl genomic DNA was prepared.

The amplification conditions were as follows: 95 °C for 5 min, 30 cycles at 94 °C for 0.5 min, 60 °C for 1 min, and 70 °C for 1 min. After the cycles, the samples were maintained at 60 °C for 0.5 min. The PCR products were separated and detected using standard procedures on a 3100 Genetic Analyzer (Applied Biosciences, Foster City, CA, USA). Cross-contamination analysis was performed by comparing allelic patterns of the P30 culture with those of the P3 culture.

DNA extraction. The hUC-MSCs were harvested at P3 (early passage) and P30 (late passage) for genomic DNA preparation. Genomic DNA was isolated using phenol–chloroform extraction. Quality and concentration of the genomic DNA were determined by electrophoresis and using a NanoDrop spectrophotometer. The genomic DNA was safeguarded from degradation and had the absorbance ratios A260/A280 of ≥1.8 and A260/A230 of ≥1.9.

Telomere length and TERT analysis. Telomere length of the hUC-MSCs was measured using the Telo*TAGGG* Telomere Length Assay Kit (Roche, Mannheim, Germany). In brief, genomic DNA was digested using a mixture of *Hin*fI and *Rsa*I, separated by gel electrophoresis, transferred to a nylon membrane for Southern blotting, hybridized to a digoxigenin-labeled probe specific for telomeric repeats, and visualized with anti-digoxigenin-AP antibody and chemiluminescence quantitation. A TaqMan-based RT-PCR assay was used to analyze *hTERT* expression. RNA was extracted from hUC-MSCs using the E.Z.N.A total RNA kit (Omega Bio-Tek, Norcross, GA, USA). Next, cDNA was synthesized using M-MLV reverse transcriptase (Invitrogen, Carlsbad, CA, USA). RT-PCR was performed using TaqMan Gene Expression Master Mix (Applied Biosystems) (*hTERT* sense primer: 5′-TGACACCTCACCTCACCCAC-3′, *hTERT* antisense primer: 5′-CACTGTCTTCCGCAAGTTCAC-3′, and the probe: 5′-ACCCTGGTCCGAGGTGTCCCTGAG-3′ with an amplicon of 95 bp) and *RPLP0* (*RPLP0* sense primer: 5′-GGCGACCTGGAAGTCCAACT-3′, *RPLP0* antisense primer: 5′-CCATCAGCACCACAGCCTTC-3′, and the probe: 5′-ATCT GCTGCATCTGCTTGGAGCCCA-3′ with an amplicon of 149 bp).[43]

Karyotype analysis. The hUC-MSCs were cultured in the presence of colcemid overnight. Next, the cells were resuspended in a prewarmed 0.075 M KCl hypotonic solution and incubated at 37 °C for 10 min. After centrifugation (1000 r.p.m., 5 min), the cells were resuspended in a fixative solution (3 : 1 methanol/acetic acid). The metaphase spreads were then prepared on glass microscope slides and analyzed using R-banding.

aCGH. DNA labeling, hybridization, washing, array scanning, and data analysis were performed at CapitalBio Corporation (Beijing, China) according to the NimbleGen CGH user's guide. In brief, pairs of genomic DNA (1 μg) were labeled with a fluorescent dye Cy3 (P30) or Cy5 (P3). The samples were cohybridized to Human CNV 3 × 720K arrays (NimbleGen, Madison, WI, USA). The arrays were scanned using an MS200 scanner (NimbleGen) with 2 μm resolution, and NimbleScan software (NimbleGen) was used to extract fluorescence intensity raw data from the scanned images. The segments with a |mean log$_2$ ratio| ≥0.25 and at least five consecutive probes were classified as 'amplification' or 'deletion'.

***In vivo* tumorigenesis.** The tumorigenicity of 3 hUC-MSC clones (clone 2, clone 3, and clone 6) that contained CNVs at P30 (clone 6 contained trisomy for chromosome 10 at P30) and two clones (clone 8 and clone 9) without CNVs at P30 was evaluated in female SCID mice. The mice were inoculated *s.c.* with 500 μl Matrigel (BD Biosciences, Bedford, MA, USA) containing 4 × 10^6 hUC-MSCs (P30) (five mice for each clone). H1 cells were used as a positive control. The H1 cells were a gift from Dr. Xiao Hu (the Institute of Hematology and Hospital of Blood Diseases, Chinese Academy of Medical Science and Peking Union Medical College, Tianjin, China). Eight weeks after injection, or tumors were obvious, the SCID mice were euthanized. The tumors or the subcutaneous tissues of the injection site were fixed, sliced, and stained with hematoxylin and eosin for histological analysis.

Preparation of mRNA-Seq library and sequencing. Total RNA was extracted from three pairs of hUC-MSC clones at P3 and P30 using TRIzol reagent (Invitrogen). An mRNA library was constructed using the Illumina mRNA-Seq library preparation kit according to the manufacturer's protocol and sequenced on the Illumina Hi-Seq 2000 genome analyzer platform. We collected 4G data for further analysis.

Gene expression analysis.
Reads were processed and aligned to the UCSC human reference genome (release hg18, March 2006) using TopHat (version 1.3.3).[44] The default parameters were used, except the number of threads used to align reads was set to 5. The aligned read files produced by TopHat were processed using Cufflinks (version 1.2.1) software (Lior Pachter, Steven Salzberg, and Barbara Wold, Berkeley, CA, USA) for further analysis, including assembling transcripts, estimating their abundance, and testing for the differential expression and regulation in mRNA-Seq samples.[45] To calculate gene expression intensity, the read counts were normalized to FPKM according to gene length and total mapped reads.[46] Genes with FPKM of >1.0 in at least one among the six samples were selected for further analysis. Ten of the differentially expressed genes detected in the mRNA-Seq analysis were selected and validated by RT-PCR. Primer sequences were listed in Supplementary Table 5. SYBR Green PCR Master Mix (Applied Biosystems, Warrington, UK) was used to perform RT-PCR analysis on 7300 Real Time PCR System (Applied Biosystems).

Gene cluster analysis.
Average linkage hierarchical clustering of gene expression intensity was performed using Pearson distance to measure the distance between genes and clones. Computation and visualization were performed using heatmap plus package in R.

Ingenuity pathways analysis.
Gene interaction networks and signaling pathways were generated using IPA software (http://www.ingenuity.com/). From a list of genes with particular expression features, IPA produces networks according to its algorithm. The significance of the networks is calculated using Fisher's exact test, and the P-value is calculated using negative logarithmic transformation. The importance of nodes in networks was measured on the basis of their connectivity, and the core molecules of networks were considered as nodes that are connected with much more edges.[47]

Conflict of Interest
The authors declare no conflict of interest.

1. Maitra A, Arking DE, Shivapurkar N, Ikeda M, Stastny V, Kassauei K et al. Genomic alterations in cultured human embryonic stem cells. Nat Genet 2005; 37: 1099–1103.
2. Narva E, Autio R, Rahkonen N, Kong L, Harrison N, Kitsberg D et al. High-resolution DNA analysis of human embryonic stem cell lines reveals culture-induced copy number changes and loss of heterozygosity. Nat Biotechnol 2010; 28: 371–377.
3. Laurent LC, Ulitsky I, Slavin I, Tran H, Schork A, Morey R et al. Dynamic changes in the copy number of pluripotency and cell proliferation genes in human ESCs and iPSCs during reprogramming and time in culture. Cell Stem Cell 2011; 8: 106–118.
4. Bieback K, Brinkmann I. Mesenchymal stromal cells from human perinatal tissues: from biology to cell therapy. World J Stem Cells 2010; 2: 81–92.
5. Lu LL, Liu YJ, Yang SG, Zhao QJ, Wang X, Gong W et al. Isolation and characterization of human umbilical cord mesenchymal stem cells with hematopoiesis-supportive function and other potentials. Haematologica 2006; 91: 1017–1026.
6. Liang J, Zhang H, Hua B, Wang H, Wang J, Han Z et al. Allogeneic mesenchymal stem cells transplantation in treatment of multiple sclerosis. Mult Scler 2009; 15: 644–646.
7. Shi D, Wang D, Li X, Zhang H, Che N, Lu Z et al. Allogeneic transplantation of umbilical cord-derived mesenchymal stem cells for diffuse alveolar hemorrhage in systemic lupus erythematosus. Clin Rheumatol 2012; 31: 841–846.
8. Jiang R, Han Z, Zhuo G, Qu X, Li X, Wang X et al. Transplantation of placenta-derived mesenchymal stem cells in type 2 diabetes: a pilot study. Front Med 2011; 5: 94–100.
9. Estrada JC, Albo C, Benguria A, Dopazo A, Lopez-Romero P, Carrera-Quintanar L et al. Culture of human mesenchymal stem cells at low oxygen tension improves growth and genetic stability by activating glycolysis. Cell Death Differ 2012; 19: 743–755.
10. Ueyama H, Horibe T, Hinotsu S, Tanaka T, Inoue T, Urushihara H et al. Chromosomal variability of human mesenchymal stem cells cultured under hypoxic conditions. J Cell Mol Med 2012; 16: 72–82.
11. Bochkov NP, Voronina ES, Kosyakova NV, Liehr T, Rzhaninova AA, Katosova LD et al. Chromosome variability of human multipotent mesenchymal stromal cells. Bull Exp Biol Med 2007; 143: 122–126.
12. Redaelli S, Bentivegna A, Foudah D, Miloso M, Redondo J, Riva G et al. From cytogenomic to epigenomic profiles: monitoring the biologic behavior of in vitro cultured human bone marrow mesenchymal stem cells. Stem Cell Res Ther 2012; 3: 47.
13. Bernardo ME, Zaffaroni N, Novara F, Cometa AM, Avanzini MA, Moretta A et al. Human bone marrow derived mesenchymal stem cells do not undergo transformation after long-term in vitro culture and do not exhibit telomere maintenance mechanisms. Cancer Res 2007; 67: 9142–9149.
14. Meza-Zepeda LA, Noer A, Dahl JA, Micci F, Myklebost O, Collas P. High-resolution analysis of genetic stability of human adipose tissue stem cells cultured to senescence. J Cell Mol Med 2008; 12: 553–563.
15. Gong W, Han Z, Zhao H, Wang Y, Wang J, Zhong J et al. Banking human umbilical cord-derived mesenchymal stromal cells for clinical use. Cell Transplant 2012; 21: 207–216.
16. Buyanovskaya OA, Kuleshov NP, Nikitina VA, Voronina ES, Katosova LD, Bochkov NP. Spontaneous aneuploidy and clone formation in adipose tissue stem cells during different periods of culturing. Bull Exp Biol Med 2009; 148: 109–112.
17. Garcia S, Bernad A, Martin MC, Cigudosa JC, Garcia-Castro J, de la Fuente R. Pitfalls in spontaneous in vitro transformation of human mesenchymal stem cells. Exp Cell Res 2010; 316: 1648–1650.
18. Rosland GV, Svendsen A, Torsvik A, Sobala E, McCormack E, Immervoll H et al. Long-term cultures of bone marrow-derived human mesenchymal stem cells frequently undergo spontaneous malignant transformation. Cancer Res 2009; 69: 5331–5339.
19. Rubio D, Garcia-Castro J, Martin MC, de la Fuente R, Cigudosa JC, Lloyd AC et al. Spontaneous human adult stem cell transformation. Cancer Res 2005; 65: 3035–3039.
20. Katsanis SH, Wagner JK. Characterization of the standard and recommended CODIS markers. J Forensic Sci 2013; 58(Suppl 1): S169–S172.
21. Mendez-Ferrer S, Michurina TV, Ferraro F, Mazloom AR, Macarthur BD, Lira SA et al. Mesenchymal and haematopoietic stem cells form a unique bone marrow niche. Nature 2010; 466: 829–834.
22. Arnold K, Sarkar A, Yram MA, Polo JM, Bronson R, Sengupta S et al. Sox2(+) adult stem and progenitor cells are important for tissue regeneration and survival of mice. Cell Stem Cell 2011; 9: 317–329.
23. Mayshar Y, Ben-David U, Lavon N, Biancotti JC, Yakir B, Clark AT et al. Identification and classification of chromosomal aberrations in human induced pluripotent stem cells. Cell Stem Cell 2010; 7: 521–531.
24. Hsia TC, Liu CJ, Lin CH, Chang WS, Chu CC, Hang LW et al. Interaction of CCND1 genotype and smoking habit in Taiwan lung cancer patients. Anticancer Res 2011; 31: 3601–3605.
25. Cao Q, Kaur C, Wu CY, Lu J, Ling EA. Nuclear factor-kappa beta regulates Notch signaling in production of proinflammatory cytokines and nitric oxide in murine BV-2 microglial cells. Neuroscience 2011; 192: 140–154.
26. Reynaud D, Pietras E, Barry-Holson K, Mir A, Binnewies M, Jeanne M et al. IL-6 controls leukemic multipotent progenitor cell fate and contributes to chronic myelogenous leukemia development. Cancer Cell 2011; 20: 661–673.
27. Chen X, Niu H, Chung WH, Zhu Z, Papusha A, Shim EY et al. Cell cycle regulation of DNA double-strand break end resection by Cdk1-dependent Dna2 phosphorylation. Nat Struct Mol Biol 2011; 18: 1015–1019.
28. Han Q, Zhang X, Xue R, Yang H, Zhou Y, Kong X et al. AMPK potentiates hypertonicity-induced apoptosis by suppressing NFkappaB/COX-2 in medullary interstitial cells. J Am Soc Nephrol 2011; 22: 1897–1911.
29. Ball LM, Bernardo ME, Roelofs H, Lankester A, Cometa A, Egeler RM et al. Cotransplantation of ex vivo expanded mesenchymal stem cells accelerates lymphocyte recovery and may reduce the risk of graft failure in haploidentical hematopoietic stem-cell transplantation. Blood 2007; 110: 2764–2767.
30. Ko MS, Jung JY, Shin IS, Choi EW, Kim JH, Kang SK et al. Effects of expanded human adipose tissue-derived mesenchymal stem cells on the viability of cryopreserved fat grafts in the nude mouse. Int J Med Sci 2011; 8: 231–238.
31. Honmou O, Houkin K, Matsunaga T, Niitsu Y, Ishiai S, Onodera R et al. Intravenous administration of auto serum-expanded autologous mesenchymal stem cells in stroke. Brain 2011; 134(Pt 6): 1790–1807.
32. Ren Z, Wang J, Zhu W, Guan Y, Zou C, Chen Z et al. Spontaneous transformation of adult mesenchymal stem cells from cynomolgus macaques in vitro. Exp Cell Res 2011; 317: 2950–2957.
33. Torsvik A, Rosland GV, Svendsen A, Molven A, Immervoll H, McCormack E et al. Spontaneous malignant transformation of human mesenchymal stem cells reflects cross-contamination: putting the research field on track - letter. Cancer Res 2010; 70: 6393–6396.

34. Torsvik A, Rosland GV, Bjerkvig R. Comment to: 'Spontaneous transformation of adult mesenchymal stem cells from cynomolgus macaques in vitro' by Z. Ren et al. Exp. Cell Res. 317 (2011) 2950-2957, In Press Spontaneous transformation of mesenchymal stem cells in culture: Facts or fiction? *Exp Cell Res* 2012; **10318**: 441–443.

35. de la Fuente R, Bernad A, Garcia-Castro J, Martin MC, Cigudosa JC. Retraction: spontaneous human adult stem cell transformation. *Cancer Res* 2010; **70**: 6682.

36. Prockop DJ, Keating A. Relearning the lessons of genomic stability of human cells during expansion in culture: implications for clinical research. *Stem Cells* 2012; **30**: 1051–1052.

37. Binato R, de Souza Fernandez T, Lazzarotto-Silva C, Du Rocher B, Mencalha A, Pizzatti L *et al.* Stability of human mesenchymal stem cells during in vitro culture: considerations for cell therapy. *Cell Prolif* 2013; **46**: 10–22.

38. Tchatchou S, Burwinkel B. Chromosome copy number variation and breast cancer risk. *Cytogenet Genome Res* 2008; **123**: 183–187.

39. Speleman F, Kumps C, Buysse K, Poppe B, Menten B, De Preter K. Copy number alterations and copy number variation in cancer: close encounters of the bad kind. *Cytogenet Genome Res* 2008; **123**: 176–182.

40. Giaretti W, Pentenero M, Gandolfo S, Castagnola P. Chromosomal instability, aneuploidy and routine high-resolution DNA content analysis in oral cancer risk evaluation. *Future Oncol* 2012; **8**: 1257–1271.

41. Pfau SJ, Amon A. Chromosomal instability and aneuploidy in cancer: from yeast to man. *EMBO Rep* 2012; **13**: 515–527.

42. Jiang X, Guo F, Jia F, Jin P, Sun Z. Development of a 20-locus fluorescent multiplex system as a valuable tool for national DNA database. *Forensic Sci Int Genet* 2013; **7**: 279–289.

43. Bieche I, Nogues C, Paradis V, Olivi M, Bedossa P, Lidereau R *et al.* Quantitation of hTERT gene expression in sporadic breast tumors with a real-time reverse transcription-polymerase chain reaction assay. *Clin Cancer Res* 2000; **6**: 452–459.

44. Trapnell C, Pachter L, Salzberg SL. TopHat: discovering splice junctions with RNA-Seq. *Bioinformatics* 2009; **25**: 1105–1111.

45. Roberts A, Trapnell C, Donaghey J, Rinn JL, Pachter L. Improving RNA-Seq expression estimates by correcting for fragment bias. *Genome Biol* 2011; **12**: R22.

46. Trapnell C, Williams BA, Pertea G, Mortazavi A, Kwan G, van Baren MJ *et al.* Transcript assembly and quantification by RNA-Seq reveals unannotated transcripts and isoform switching during cell differentiation. *Nat Biotechnol* 2010; **28**: 511–515.

47. Jia Q, Zhang Q, Zhang Z, Wang Y, Zhang W, Zhou Y *et al.* Transcriptome analysis of the Zebrafish model of diamond-blackfan anemia from RPS19 deficiency via p53-dependent and -independent pathways. *PLoS One* 2013; **8**: e71782.

Supplementary Information accompanies this paper on Cell Death and Disease website (http://www.nature.com/cddis)